

# A New Procedure for Simultaneous Navigation of Multiple AUV's

**Bradley N. Baker**

Department of Mechanical Engineering, University of Idaho, Moscow, ID 83844-0902

**Douglas L. Odell**

CDNSWC Acoustic Research Detachment, 33890 North Main Street, Bayview, ID 83803

**Michael J. Anderson**

Department of Mechanical Engineering, University of Idaho, Moscow, ID 83844-0902

**Thomas A. Bean**

Department of Mechanical Engineering, University of Idaho, Moscow, ID 83844-0902

**Dean B. Edwards**

Department of Mechanical Engineering, University of Idaho, Moscow, ID 83844-0902

**Abstract** - Navigation by Underwater Autonomous Vehicles (AUV's) is a challenging problem because radio waves do not penetrate water, and acoustic waves must be used instead for determination of position. Current systems utilize round-trip time-of-flight between single vehicles and fixed transponders to determine position. While reliable, the drawback of this method is that there is an upper limit on the number of vehicles that can navigate at the same time. We describe a new procedure that allows simultaneous navigation of multiple vehicles using the acoustic navigation signals from only one vehicle in the group. One vehicle in the group is assigned to navigate conventionally with an acoustic Long BaseLine (LBL) system. The other vehicles in the group are equipped with a sensor that can determine the relative angular heading to the source of an intercepted acoustic signal, and a separate sensor that can determine angular inertial heading. As the chosen vehicle navigates conventionally, the other vehicles in the group intercept the return pings from the fixed transponders. From these signals, and the inertial heading, each vehicle is able to determine their inertial position. The sensor used to determine relative angular heading to the source of an intercepted signal consists of two hydrophones separated by an approximate distance of one meter. Relative angular heading is extracted from the difference-in-arrival time using correlation between the hydrophone signals. An error propagation analysis is performed that quantifies the accuracy of the inertial position fix as it depends upon vehicle-transponder geometry, and sensor precision. Experiments, designed to determine the accuracy of the navigation technique to compare with error-propagation analysis, and to explore its performance when implemented in formation-flying cooperative behavior, are described.

## I. INTRODUCTION

In the future, it is thought that large numbers of Autonomous Underwater Vehicles (AUV's) may be used to perform tasks that would take too long for small numbers of AUV's to undertake. An example would be to search or patrol a large area.

At least two problems must be solved to employ large numbers of AUV's to complete the task. The first is to enable cooperative behaviors, so that the need for human supervision is minimized. Formation-flying has been proposed [1] as one fundamental behavior that would enable other cooperation. The second problem is that large numbers of vehicles must navigate simultaneously in order to complete a task in a reasonable time period. Most

AUV's presently use an acoustic Long BaseLine (LBL) system similar to that described in [2] for underwater navigation. This type of system determines position using round-trip time-of-flight data from acoustic pings exchanged between a vehicle and two or more transponders at known locations. Although this approach is reliable, each vehicle navigates individually, which places an upper limit on the number of vehicles that could navigate at the same time.

In this paper, we explore the feasibility of an alternate system for underwater navigation. This system combines features of formation-flying cooperation and simultaneous underwater navigation. A leader vehicle performs tasks with a fleet of follower vehicles. The lead vehicle would navigate conventionally using acoustic LBL transponders. Each follower vehicle would intercept acoustic navigation signals from the leader and the LBL transponders with a two-hydrophone sensor [3]. This sensor would be used to determine the bearing angle to the leader vehicle and the transponders. Assuming that the follower vehicles are equipped with a sensor capable of measuring inertial heading, it is then possible for the follower vehicles to determine their inertial position.

## II. POSITION DETERMINATION ALGORITHM

Consider the relative geometry of a leader and follower vehicle and fixed transponders shown in Fig. 1. Fig. 1 is a top view and  $(x,y)$  measures the inertial position. It is assumed that the fixed transponders and vehicles are at the same depth  $z$ . Fixed transponders, labeled  $T_1$  and  $T_2$ , are located at  $(x_1,y_1)$  and  $(x_2,y_2)$  respectively. A follower vehicle is located at  $(x^*,y^*)$ . The inertial heading of the follower vehicle, and the bearing angles to transponders  $T_1$ ,  $T_2$ , the leader vehicle are  $\beta$ ,  $\sigma_1$ ,  $\sigma_2$ , and  $\sigma_l$  respectively. It is assumed that the bearing angles  $\sigma_1$ ,  $\sigma_2$ , and  $\sigma_l$  can be measured with the two-hydrophone sensor, and that the inertial heading  $\beta$  can be measured with an appropriate sensor on the follower vehicle.

By constructing a triangle of vectors connecting the points  $(x_1,y_1)$ ,  $(x_2,y_2)$  and  $(x^*,y^*)$ , it is possible to derive two formulas that relate the measured bearing angles  $\sigma_1$  and  $\sigma_2$  and the inertial heading  $\beta$  to the position  $(x^*,y^*)$  of the vehicle. These formulas are

$$x^* = x_1 + d \cos(\sigma_1 + \beta) \frac{\sin \phi \cos(\sigma_2 + \beta) - \cos \phi \sin(\sigma_2 + \beta)}{\sin(\sigma_1 + \beta) \cos(\sigma_2 + \beta) - \sin(\sigma_2 + \beta) \cos(\sigma_1 + \beta)},$$

Report Documentation Page			Form Approved OMB No. 0704-0188		
Public reporting burden for the collection of information is estimated to average 1 hour per response, including the time for reviewing instructions, searching existing data sources, gathering and maintaining the data needed, and completing and reviewing the collection of information. Send comments regarding this burden estimate or any other aspect of this collection of information, including suggestions for reducing this burden, to Washington Headquarters Services, Directorate for Information Operations and Reports, 1215 Jefferson Davis Highway, Suite 1204, Arlington VA 22202-4302. Respondents should be aware that notwithstanding any other provision of law, no person shall be subject to a penalty for failing to comply with a collection of information if it does not display a currently valid OMB control number.					
1. REPORT DATE <b>2005</b>		2. REPORT TYPE		3. DATES COVERED <b>00-00-2005 to 00-00-2005</b>	
4. TITLE AND SUBTITLE <b>A New Procedure for Simultaneous Navigation of Multiple AUV's</b>			5a. CONTRACT NUMBER		
			5b. GRANT NUMBER		
			5c. PROGRAM ELEMENT NUMBER		
6. AUTHOR(S)			5d. PROJECT NUMBER		
			5e. TASK NUMBER		
			5f. WORK UNIT NUMBER		
7. PERFORMING ORGANIZATION NAME(S) AND ADDRESS(ES) <b>University of Idaho, Department of Mechanical Engineering, Moscow, ID, 83844</b>			8. PERFORMING ORGANIZATION REPORT NUMBER		
9. SPONSORING/MONITORING AGENCY NAME(S) AND ADDRESS(ES)			10. SPONSOR/MONITOR'S ACRONYM(S)		
			11. SPONSOR/MONITOR'S REPORT NUMBER(S)		
12. DISTRIBUTION/AVAILABILITY STATEMENT <b>Approved for public release; distribution unlimited</b>					
13. SUPPLEMENTARY NOTES <b>The original document contains color images.</b>					
14. ABSTRACT					
15. SUBJECT TERMS					
16. SECURITY CLASSIFICATION OF:			17. LIMITATION OF ABSTRACT	18. NUMBER OF PAGES <b>4</b>	19a. NAME OF RESPONSIBLE PERSON
a. REPORT <b>unclassified</b>	b. ABSTRACT <b>unclassified</b>	c. THIS PAGE <b>unclassified</b>			

$$y^* = y_1 + d \sin(\sigma_1 + \beta) \frac{\sin \phi \cos(\sigma_2 + \beta) - \cos \phi \sin(\sigma_2 + \beta)}{\sin(\sigma_1 + \beta) \cos(\sigma_2 + \beta) - \sin(\sigma_2 + \beta) \cos(\sigma_1 + \beta)}, \quad (1a, 1b)$$

and

$$x^* = x_2 + d \cos(\sigma_2 + \beta) \frac{\sin \phi \cos(\sigma_1 + \beta) - \sin(\sigma_1 + \beta) \cos \phi}{\sin(\sigma_1 + \beta) \cos(\sigma_2 + \beta) - \sin(\sigma_2 + \beta) \cos(\sigma_1 + \beta)},$$

$$y^* = y_2 + d \sin(\sigma_2 + \beta) \frac{\sin \phi \cos(\sigma_1 + \beta) - \sin(\sigma_1 + \beta) \cos \phi}{\sin(\sigma_1 + \beta) \cos(\sigma_2 + \beta) - \sin(\sigma_2 + \beta) \cos(\sigma_1 + \beta)}, \quad (2a, b)$$

where  $d=d(x_1, y_1, x_2, y_2)$  is the distance between the fixed transponders  $T_1$  and  $T_2$ , and  $\phi=\phi(x_1, y_1, x_2, y_2)$  is the angular orientation of transponder  $T_2$  relative to transponder  $T_1$ . The sets (1,2) are derived by computing the position of the vehicle relative to fixed transponders  $T_1$  and  $T_2$  respectively.

The precision of the determination of inertial position  $(x^*, y^*)$  using (1) or (2) can be estimated using root-sum-square error propagation [4]. Supposing that the quantities  $x_1, y_1, x_2, y_2, \sigma_1, \sigma_2$  and  $\beta$  are known to a precision of  $\epsilon_{x1}, \epsilon_{y1}, \epsilon_{x2}, \epsilon_{y2}, \epsilon_{\sigma1}, \epsilon_{\sigma2}, \epsilon_{\beta}$ , then the uncertainty  $\epsilon_{x^*}$  on the determination of  $x^*$  can be estimated with

$$\epsilon_{x^*}^2 \approx \left( \frac{\partial x^*}{\partial x_1} \epsilon_{x1} \right)^2 + \left( \frac{\partial x^*}{\partial y_1} \epsilon_{y1} \right)^2 + \left( \frac{\partial x^*}{\partial x_2} \epsilon_{x2} \right)^2 + \left( \frac{\partial x^*}{\partial y_2} \epsilon_{y2} \right)^2 + \left( \frac{\partial x^*}{\partial \sigma_1} \epsilon_{\sigma1} \right)^2 + \left( \frac{\partial x^*}{\partial \sigma_2} \epsilon_{\sigma2} \right)^2 + \left( \frac{\partial x^*}{\partial \beta} \epsilon_{\beta} \right)^2. \quad (3)$$

A similar expression can be derived for an estimate of the uncertainty  $\epsilon_{y^*}$  on the coordinate  $y^*$ . In an actual application, the uncertainty propagated to  $\epsilon_{x^*}$  from  $\epsilon_{x1}, \epsilon_{y1}, \epsilon_{x2}, \epsilon_{y2}$  would appear as bias, while those propagated by  $\epsilon_{\sigma1}, \epsilon_{\sigma2}, \epsilon_{\beta}$  would contribute to uncertainty in precision.

### III. EXPERIMENTS AND APPARATUS

Tests were conducted in freshwater on lake Pend Oreille at the Acoustic Research Detachment [5]. The test area was approximately 300 m from shore in depths varying from 10 m to 35 m. Acoustic navigation transponders were placed 146 m (480 ft) apart near the periphery of the test area, each at a depth of 12 m. During warmer summer months, thermal gradients develop near the surface. Sound speed measurements on the day of testing showed sound velocity of 1448 m/s (4750 ft/s) nearest the surface, slowing to 1426 m/s (4680 ft/s) near the bottom. The steepest velocity gradient was within the upper 2m of water, with a value of 13 m/s per meter of depth change. The increased sound velocity in shallower water causes horizontal acoustic ray paths to bend downward [6]. This creates acoustic shadow zones near the surface in which acoustic power diminishes very rapidly as the horizontal separation between source and receiver increases.

The acoustic source and two-hydrophone receiver were suspended below two surface craft, 7.3 m (24 ft) foot utility boats with outboard engines, at an approximate depth of 2 meters. The boats traveled at speeds of 1-2 m/s and maintained a separation of 20-40 m. Trajectory controllers directed human operators to drive the boats along prescribed paths, described by sets of waypoints, by

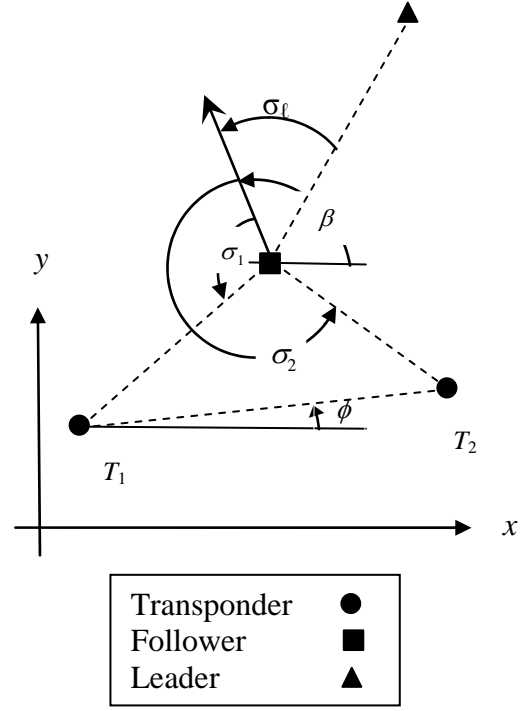


Fig. 1 Vehicle and transponder geometry.

displaying the recommended rudder position and desired velocity on a computer screen. The lead boat held a constant velocity throughout the tests while the following boat varied its throttle to maintain the desired orientation. The positions of the boats were measured with a Global Positioning System (GPS), and the follower boat received the leader boat's position either by direct communication via a Woods Hole acoustic micro-modem [2], or by inferring it as the intersection of the waypoint path and the relative angle discussed above. The following distance between the two vehicles was calculated by projecting the displacement vector, from the follower to the leader, onto the following vehicle's desired heading vector using vector algebra. This following distance was then compared to a reference distance to arrive at the following distance error. A dead-bang type controller was designed to find the following boat's desired velocity.

The Woods Hole modem was used to drive the source transmitter. The source transducer was omni-directional, broadband, with a resonant frequency of 32 kHz (ITC-1032). The source amplitude level was 183 dB (re 1  $\mu$ Pa @ 1yd). The source emitted a BPSK navigation ping generated by the Woods Hole modem having a carrier frequency of 26 kHz, nominal bandwidth of 4 kHz, and duration of 7 ms. Two portable acoustic transponders were deployed at fixed locations within the test area and interact with the modem for navigation purposes. The hydrophones used in the two-hydrophone sensor were omnidirectional, had a flat frequency response from 1-40kHz and approximate sensitivity of -165dB V/Pa (ITC-8140). The separation distance between the two hydrophones was 0.457 m (18 in). The hydrophone voltage signals were anti-alias filtered and sampled simultaneously with 16-bit resolution at a sample rate of 65536 Hz.

Bearing angles were determined with the two-hydrophone sensor using the signal arrival time

difference  $\Delta t$  extracted from the hydrophone signals. The difference in arrival time  $\Delta t$  from the two hydrophone signals was extracted using a cross-correlation method. This procedure is similar to that used to extract time-of-flight using matched filter processing [5], except that two measured signals were used in this procedure, as opposed to a measured signal and pre-generated noise-free replica waveforms. The cross-correlation approach allows simpler and in some ways more robust processing. Prior to correlation, leading-edge detection was used to generally locate the transmitted acoustic signal within each hydrophone data stream. Each hydrophone signal was then translated to baseband with a complex sinusoid. A real, symmetric FIR low-pass filter was applied to remove out-of-band interference (such as engine noise). The resulting analytic signals were then cross-correlated producing a sampled complex correlation output. The desired delay time  $\Delta t$  was extracted by maximizing the cross-correlation amplitude. To minimize sample-interval round-off errors, a sinc interpolation procedure [7] was used to fit several points surrounding the sampled peak.

#### IV. RESULTS AND DISCUSSION

##### A. Precision of Position Determination Algorithm

An example computation of the precision  $\varepsilon_{x^*}$  and  $\varepsilon_{y^*}$  in position determination for a specific example is contained in Fig. 2. In this example, the transponders  $T_1$  and  $T_2$  were located 500m apart, at  $(x_1, y_1) = (-250, 0)$ m and  $(x_2, y_2) = (250, 0)$ m respectively. It was assumed that the uncertainties on the measurements of  $x_1, y_1, x_2, y_2, \sigma_1, \sigma_2$  and  $\beta$  were  $\varepsilon_{x_1} = \varepsilon_{y_1} = \varepsilon_{x_2} = \varepsilon_{y_2} = 2$ m,  $\varepsilon_{\sigma_1} = \varepsilon_{\sigma_2} = \varepsilon_{\beta} = 1^\circ$  respectively. At each location  $(x^*, y^*)$ , it was further assumed that the inertial heading of the vehicle was  $\beta = 0^\circ$ . In the computations, the vehicle was placed at positions  $(x^*, y^*)$  ranging from  $-1000\text{m} < x^* < 1000\text{m}$  and  $-1000\text{m} < y^* < 1000\text{m}$ , and the resulting uncertainties  $\varepsilon_{x^*}$  and  $\varepsilon_{y^*}$  were computed and plotted as a surface in the upper and lower parts of Fig. 2 respectively. The surfaces have been truncated at 30 m to retain detail for smallest uncertainties.

In the example considered, the precision of position determination using the set (1) was about 10m on the  $x^*$  and  $y^*$  within a rectangle bounding the fixed transponders. Precision was rapidly lost on both  $x^*$  and  $y^*$  outside this rectangle. This behavior would be expected when using bearing angle to predict position at greater distances. Precision was also lost for the coordinate  $x^*$  on a line connecting the fixed transponders. When the vehicle was on this line, the perturbations in the bearing angles did not contain any information about corresponding perturbations in the  $x^*$  coordinate of the vehicle. This example shows that the use of the procedure (1) for position determination would be limited to small areas near the fixed transponders.

There are reasons to believe that the position determination procedures (1,2) may be augmented by other information in the signals received by the two-hydrophone sensors that could be used to improve the precision of the position estimate. For example, one could exploit the fact that the hydrophone signals contain two independent estimates of the arrival time difference  $\tau$  between the return pings from the two fixed transponders. Use of this information has been termed passive navigation [2]. This

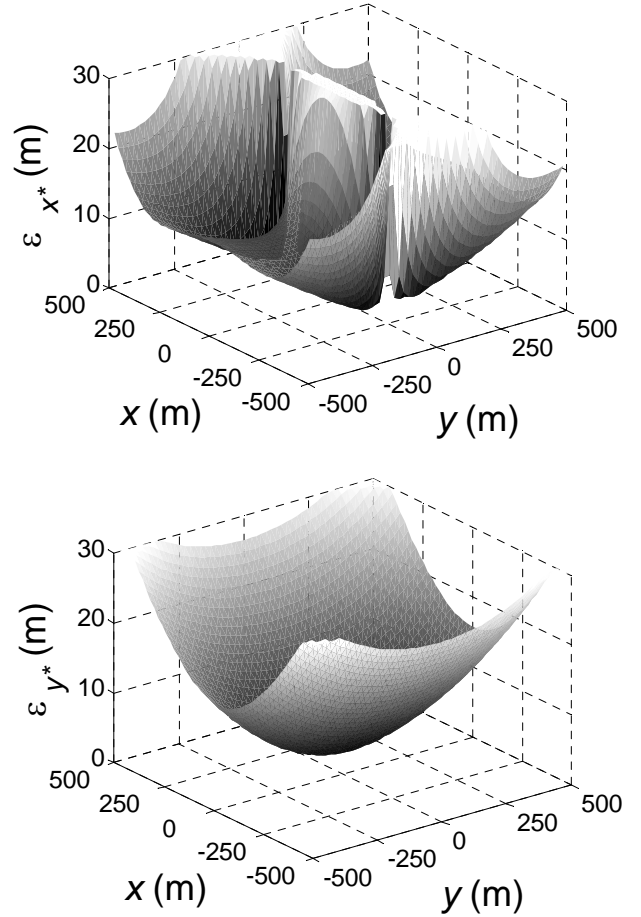


Fig. 2. Uncertainty propagated to the  $x^*$  and  $y^*$  coordinates of follower vehicle.

constraint could be added to the set (1,2), and, hypothetically, improve the precision on the determination of  $(x^*, y^*)$ .

##### B. Experimental Measurements of Bearing Angles

Experimental measurements of bearing angles  $\sigma_1, \sigma_2$ , and  $\sigma_\ell$  are shown in Fig. 3. The horizontal axes on Figure 3 measure the elapsed time during a formation-flying maneuver by the two surface craft. The bearing angles  $\sigma_1, \sigma_2$ , and  $\sigma_\ell$  are marked with open circles. For comparison, indicated bearing angles were computed from GPS position data. For example, an indicated bearing angle to the leader  $\phi_\ell$  was computed from GPS data using

$$\phi_\ell = \beta - \tan^{-1} \left( \frac{y^* - y_\ell}{x^* - x_\ell} \right). \quad (4)$$

Similar expressions were used to compute indicated bearing angles  $\phi_1$  and  $\phi_2$  to compare with measured bearing angles  $\sigma_1$  and  $\sigma_2$ . The indicated bearing angles are denoted in Fig. 3 with the cross (x) symbol.

The error bars in Fig. 3 quantify the uncertainty associated with bearing angle measurement. The uncertainty for indicated bearing angle  $\phi_\ell$  to the leader vehicle was computed using root-sum square error propagation applied to (4). The uncertainty on the indicated bearing angles  $\phi_1$  and  $\phi_2$  for transponders  $T_1$  and  $T_2$  were calculated in the same manner. For these calculations, it was assumed that the uncertainty on the GPS position measurement was 1m. The uncertainty of the two-hydrophone sensor was assumed to be  $\pm 3^\circ$ .

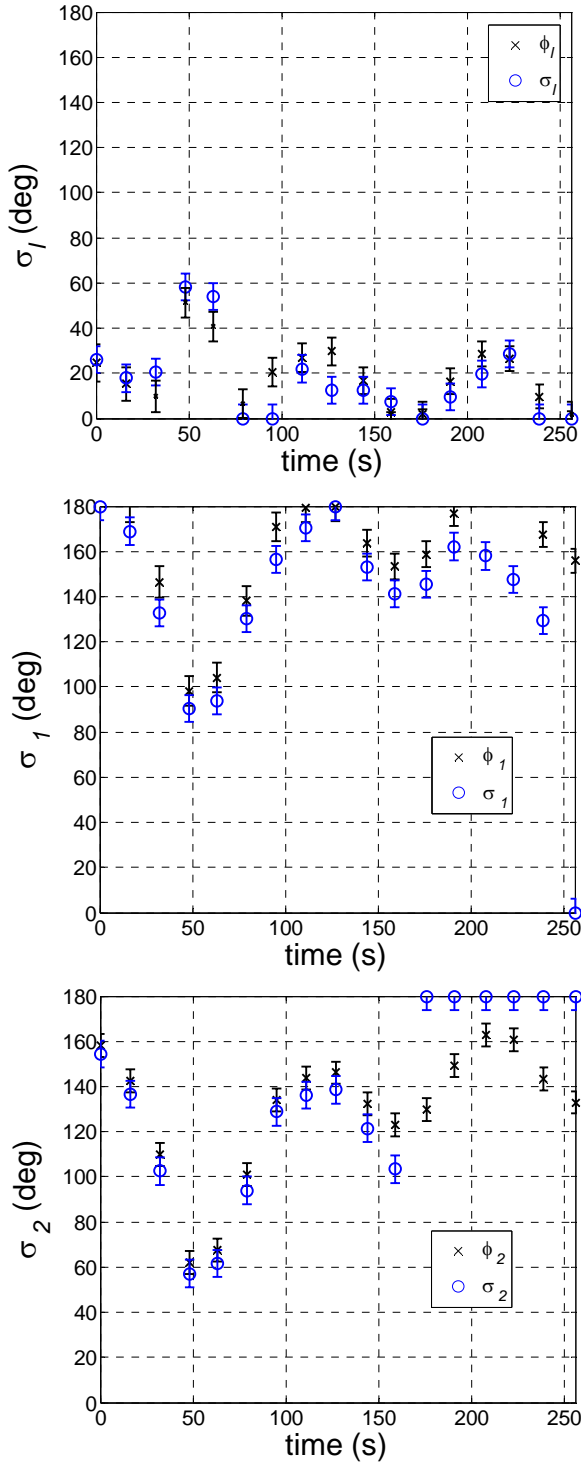


Fig. 3 Bearing angles to leader and fixed transponders as determined by follower two-hydrophone sensor and GPS data.

With some exceptions, there was agreement of measured bearing angles  $\sigma_1$ ,  $\sigma_2$ , and  $\sigma_\ell$  and the indicated bearing angles  $\phi_1$ ,  $\phi_2$  and  $\phi_\ell$  within the assumed uncertainty. One cause of disagreement was the failure of the two-hydrophone sensor to determine a bearing angle. This situation occurred several times for the determination of the bearing angle to transponder  $T_2$  for  $t > 150$  s. During this time period, the follower vehicle was at maximum distance from the transponders, and it was thought that the transponder signal was lost due to the thermocline. Other isolated disagreements can be caused by improper

correlation to surface bounce, which has been observed to occur occasionally with the two-hydrophone sensor [3].

## V. CONCLUSIONS

The navigation scheme proposed in this paper has shown potential in allowing for a large number of AUV's to navigate simultaneously. Analysis of uncertainty propagated to position determination in a specific example showed a precision of 10m within a square area 500m×500m, and that precision was rapidly lost outside this area. Experimental measurements of bearing angles to fixed transponders and a leader vehicle using a two-hydrophone sensor agreed with those computed from GPS position measurements. It is thought that other information in the hydrophone signals, as yet unused, could be applied to improve the precision of the navigation procedure.

## Acknowledgments

The authors gratefully acknowledge the support of the Office of Naval Research under the award "Developing Fleets of Autonomous Underwater Vehicles" No. N00014-05-1-0674. Help with graphics and error propagation computations, provided by Jesse Kappmeyer, was also greatly appreciated.

## REFERENCES

- [1] D. B. Edwards, T. Bean, D. Odell, M.J. Anderson, "A leader-follower algorithm for multiple AUV formations", *Proceedings of 2004 IEEE/OES Autonomous Underwater Vehicles*, Sebasco Estates, Maine – June 17-18, 2004.
- [2] L. Freitag, M. Johnson, M. Grund, S. Singh, and J. Presig, "Integrated acoustic communication and navigation for multiple UUV's", *Oceans Conference Record (IEEE)*, Vol. 4, pp. 2065-2070, 2001.
- [3] C. Reeder, A. Okamoto, M. Anderson, D. Edwards, "Two-hydrophone heading and range sensor applied to formation-flying for underwater AUV's", *Oceans'04 Techno-Ocean'04 (OTO'04) Conference Proceedings*, pp. 517-523, 2004.
- [4] J.P. Holman, *Experimental Methods for Engineers*, 3<sup>rd</sup> Edition, McGraw Hill, 1978.
- [5] D. Odell, K. Hertel, C. Nelson, "New acoustic systems for AUV tracking, communications, and noise measurements at NSWCCD-ARD, lake pend oreille, Idaho", *Oceans Conference Record (IEEE)*, Vol. 1, pp. 266-271, 2002.
- [6] W.S. Burdic, *Underwater acoustic systems analysis*, Prentice-Hall, 1984.
- [7] L.C. Ludeman, *Fundamentals of Digital Signal Processing*, Harper & Row, 1986.